EPJ Web of Conferences **67**, 02032 (2014)
DOI: 10.1051/epjconf/20146702032

Modelling of airflow in a closed simulation box with regard to atmospheric optical link

Lukas Hajek[1a], Jan Latal[1a], Marian Bojko[2], Radek Poboril[1], Petr Koudelka[1], Jan Vitasek[1], Petr Siska[1], Vladimir Vasinek[1]

[1] Department of Telecommunications, Faculty of Electrical Engineering and Computer Science, VSB-Technical University of Ostrava, 17.listopadu 15, Ostrava-Poruba, 708 33, Czech Republic
[2] Department of Hydrodynamics and Hydraulic Equipment, Faculty of Mechanical Engineering, VSB-Technical University of Ostrava, 17.listopadu 15, Ostrava-Poruba, Czech Republic

Abstract. Article is dealing with defining of mathematical turbulent air flow numerical model in the laboratory box with help of ANSYS Fluent software application. The paper describes real measurement of parameters of mechanical turbulences created by high-speed ventilator mounted on the simulation box. The real measurement took place in two planes perpendicular to each other, input and output slot. Subsequently the simulation of mechanical air flow was performed by the help of k-ε and k-ω turbulent models. The results of individual simulations were evaluated by statistical model in the same points, planes respectively, in which the real measurement was made. Other simulation was dealing with effect of heaters inside of closed laboratory box with regards to optical beam degradation. During real measurement was performed temperature point measurement by probe placed inside of the box. The probe was recording air temperature every one second during seven minutes long measurement. The results comparison of simulated and measured data was made in the end. The maximal temperature reached approximately 50 °C in both cases. Also the air flow character in dependence on the number of hot-air extraction ventilators was monitored.

1 Introduction

The current trend of information transmission is moving towards an optical communication systems. The fiber optic systems replace the current cable communications because of its advantages and recently wireless optical links are used more often. These communication systems use a laser source that generates electromagnetic waves with Gaussian intensity distribution in the plane perpendicular to the propagation direction [1], [2], [3].

The atmosphere has a negative effect on the transmission of information in the form of optical beams. Phenomena such as wind turbulence, absorption, aerosol, mist, insects or birds can cause a decline or disappearance of the signal level or change of the beam spatial coherence. For this reason is necessary thoroughly study of location where is wireless optical link installed to prevent or reduce the degrading influence of the environment on the optical beam [1], [2], [3]. This paper deals possibility of using simulation software ANSYS Fluent 14, which is used for simulating fluid dynamics by using finite volume method (FVM) for numerical modeling of turbulent flow.

The basic idea is to compare the simulated and measured data of air flow velocity or temperature change in the environment of the simulation box.

2 Scheme of the simulation box

The real experiments took place in simulation box produced not only for the purpose of testing the effect of turbulent flow but also influence of fog on the optical beam. Simulation box shown on figure 1 is made of Plexiglas. Box can be completely closed, or the lid of the box can be removed, which was used in the simulation of turbulent flow. Each side of simulation box contains three holes that can be fitted with fans, left empty or closed by the lid.

3 Characteristics of the mathematical model

The flow of fluids (gases and liquids) is divided into laminar and turbulent flow. To determine the nature of flow is used dimensionless parameter called the Reynolds number:

$$\mathrm{Re} = \frac{v \cdot d_h}{\nu}, \qquad (1)$$

where d_h (m) describes the characteristic diameter equal to the diameter of the inlet hole, v (m·s^{-1}) velocity of air flow and ν (m^2·s^{-1}) kinematic viscosity of flowing media.

[a] Corresponding authors: jan.latal@vsb.cz, lukas.hajek@vsb.cz

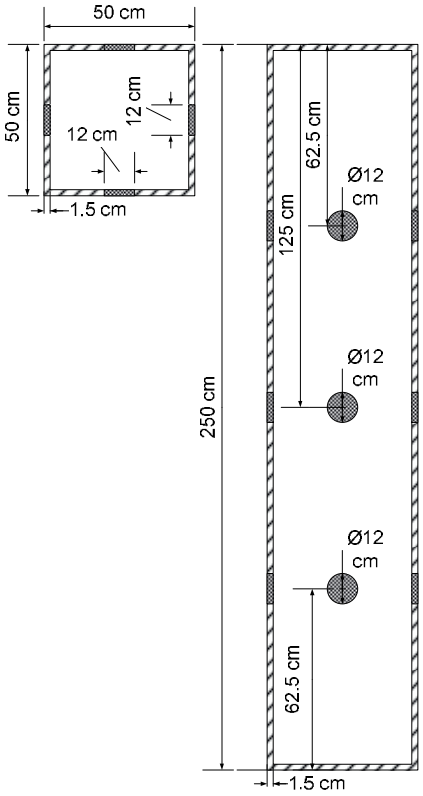

Figure 1. Schematic layout of the simulation box.

Type of flow can be determined from the size of the Reynolds number. For determining the boundaries between laminar and turbulent flow is discovered many values, which may vary depending on the pressure, altitude, or a temperature. Approximately is took into consideration the relationship $2300 < Re < 4000$, where the $Re < 2300$ is the laminar flow and at $Re > 4000$ is the turbulent flow. The area between them is known as the transition region [4].

As a laminar flow is considered to fluid flow of such a viscosity that the streamlines does not mix and are parallel to the propagation direction of the medium. This type of flow can be observed for example in liquids at low speeds and high viscosity. On the contrary, turbulent flow shows chaotic changes (fluctuations) in case of temperature, pressure, speed and direction of flow [4].

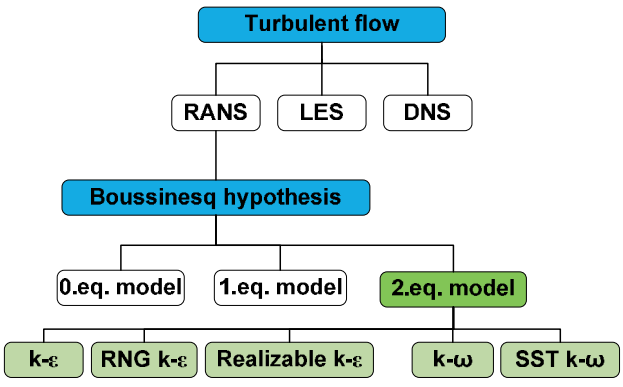

Figure 2. Numerical models [4].

The turbulent flow can be modeled by multiple methods that are developed especially with the increasing computing power of today's computers. The basic techniques include simulations of large eddies (LES) or direct numerical simulation (DNS). However, the DNS method becomes technically unfeasible because of the growing complexity of models, size of computational net and Reynolds number. One of the most used methods today is the Reynolds averaging of the Navier-Stokes equations (RANS). This method is based on the time-averaged values of turbulent flow and time-averaging procedure at balance equations [5], [7].

$$\zeta = \overline{\zeta} + \zeta' \tag{2}$$

$$\overline{\zeta} = \frac{1}{T}\int_0^T \zeta dt,\ \overline{\zeta'} = 0 \tag{3}$$

Individual immediate values of the turbulent flow (ζ) are divided into the sum of the median value $(\overline{\zeta})$ and fluctuating value (ζ').

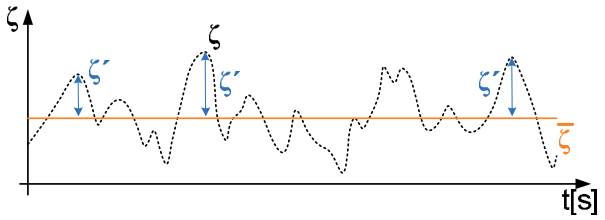

Figure 3. Mean, fluctuation, immediate value [2].

Meanwhile, the median value is the arithmetic average in a specific period T and the average value of fluctuations is equal to zero (see equation (3)). Based on equation (2) and (3) the equation of continuity (4) and N-S equation (5) of incompressible, time-independent flow can be defined into the form:

$$\frac{\partial \overline{u}_j}{\partial x_j} = 0, \tag{4}$$

$$\frac{\partial(\overline{u}_i \cdot \overline{u}_j)}{\partial x_j} + \frac{\partial(\overline{u'_i \cdot u'_j})}{\partial x_j} = -\frac{1}{\rho}\frac{\partial(\overline{p})}{\partial x_i} + \nu\frac{\partial^2(\overline{u_i})}{\partial x_j^2} + \overline{f_i}\,. \tag{5}$$

After adjustment of the N-S equations, the tensor of Reynolds (turbulent) stress arises in the link (5), the tensor must be numerically modeled. So that the demands on the calculation of the turbulent flow weren't high enough, the Boussinesq hypothesis was introduced. The hypothesis uses Newtonian relation to replace the tensor of nine shear stresses with one quantity on the same unit as that one of the dynamic viscosity. The result of Boussinesq hypothesis is modified N-S equation for compressible, time-independent flow:

$$\frac{\partial(\overline{u}_i \cdot \overline{u}_j)}{\partial x_j} = -\frac{1}{p}\frac{\partial(\overline{p})}{\partial x_i} + \nu_{eff}\frac{\partial^2(\overline{u}_i)}{\partial x_j^2} + \overline{f_i}\,. \tag{6}$$

Boussinesq hypothesis is the basis of the numerical models that have lower computational requirements during calculating of the turbulent viscosity. The division into zero, one and two-linear equation models is represented on the picture 2.

Zero-linear equation model refers to the fact that apart from the equation of conservation of energy, momentum and mass no transport equations are needed. Next is single linear equation model, which uses a transport equation for modeling the turbulent kinetic energy that is a function of the turbulent viscosity. However is necessary to specific the turbulent rule which is dependent on the qualities of the flow. The zero-linear and one-linear equation models are called incomplete models because it is necessary to know the character of the flow during the calculation of these models. When modeling the turbulent flow, the two-linear equation models k-ω a k-ε [6] are defined the most often.

The models which are used in this work are the two-linear equation models: k-ε Standard, k-ε RNG, k-ε Realizable, k-ω Standard a k-ω SST.

4 Peripheral conditions

The definition of peripheral conditions (velocity, pressure, flow) is the basis while designing a variant of numerical simulations that were made by program ANSYS Fluent 14.0 [6]. These conditions determine the basic entrance parameters which influence the result of the whole simulation. It is very important to set the peripheral conditions so that they respond to the real values the most exactly.

4.1 Numerical simulations of the turbulent flow in the box.

At this simulation of turbulent flow, the temperature isn't important parameter, therefore it is considered as neglected.

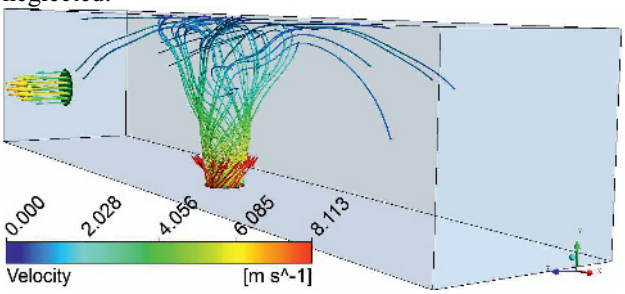

Figure 4. Input boundary conditions.

The most substantial part at the setting the peripheral conditions was focused on entrance opening. It was very important to keep identical parameters with the real model as the most precisely as possible. On the picture 4, there is the setting of entrance peripheral condition which copies the whirling flow behavior of the generated media by the rotor vanes of the entrance ventilator that is located on the lower side in the middle of the box. It was a ventilator SUNON A2123-HBT. The red-marked vectors (picture 4) determine the direction of the entrance flow. The maximal value of the air rate of flow is set by producer on 117 CFM, which corresponds the volumetric air flow Qv = 0.05427 $m^3 \cdot s^{-1}$. The final mass flow rate Qm [$kg \cdot s^{-1}$] is the result of the multiplication the volumetric flow Qv and air density ρ = 1.25 $kg \cdot m^{-3}$:

$$Q_m = Q_v \cdot \rho = 0.06784\ kg \cdot s^{-1} \quad (7)$$

The turbulent intensity I [%] on input is expressed by the size of Reynolds number [6].

$$I = 0.16 \cdot (\mathrm{Re})^{-1/8} = 0.16 \cdot (25139)^{-1/8} = 4.5\% \quad (8)$$

The air is sucked into the box by the ventilator that is composed of the firm stator and moving rotor part containing vanes. Therefore the ring is the entrance area which corresponds to the hydraulic diameter of the entrance peripheral condition. This dimension is the difference between the outer part (12 cm) and the inner stator part (4.5 cm).

Table 1. Boundary conditions.

Input b.c.	**Type**		Mass-flow-inlet
	Mass flow rate [$kg \cdot s^{-1}$]		0.06784
	Turbulent intensity [%]		4.5
	Hydraulic Diameter [m]		0.075
	Coordinate System -Local Cylindrical (Radial, Tangential, Axial)		Radial = 0
			Tangential = 1
			Axial = 1
	Axis Origin (x,y,z) [m]		(1.25 , 0 , 0.25)
	Axis Direction (x,y,z)		(0, 1, 0)
Output b.c.	Pressure-outlet		Zero pressure
Materials-Fluid	air	Density [$kg \cdot m^{-3}$]	1.225
		Cp [$J \cdot kg^{-1} \cdot K^{-1}$]	1006.43
		Thermal Conductivity [$W \cdot m^{-1} \cdot K^{-1}$]	0.0242
		Viscosity [$kg \cdot m^{-1} \cdot s^{-1}$]	1.789e-05

4.2 Turbulent flow with the temperature transfer

At the turbulent flow realization with the temperature transfer, the basic model topology was changed by the displacement of the model 335 mm along the axis Y. Under the major box model, there is a new volume representing free space between the lower side of box and the exit of hot-air ventilator (red-marked part on the picture 5). The exit opening which is located on the top side of box was provided with ventilator that sucked hot air out of the box.

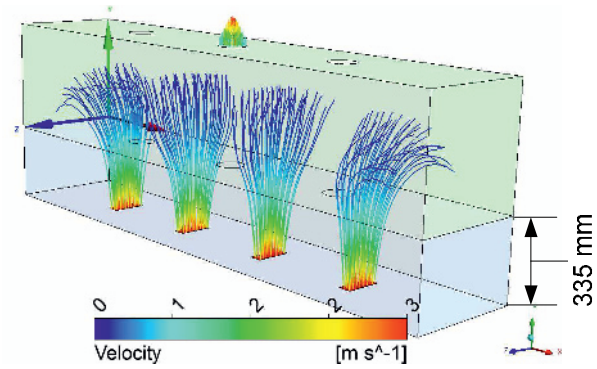

Figure 5. Input boundary conditions.

Table 2. Boundary conditions.

Hot-air ventilators	**Type**		Velocity-inlet
	Velocity magnitude [m·s^{-1}]		3
	Temperature [K]		520
Output b.c.	**Type**		Mass-flow-inlet
	Mass flow rate [kg·s^{-1}]		0.06784
	Turbulent intensity [%]		4.5
	Hydraulic Diameter [m]		0.075
Materials-Fluid	air	Density [kg·m^{-3}]	1.225
		Cp [J·kg^{-1}·K^{-1}]	1006.43
		Thermal Conductivity [W·m^{-1}·K^{-1}]	0.0242
		Viscosity [kg·m^{-1}·s^{-1}]	1.789e-05

5 Measuring and evaluation of flow field

5.1 Procedure and measuring results

The measuring device (turbine anemometer) which evaluates instantaneous value of the flow speed was used for measuring speed field in the laboratory box. The measuring was realized in the box in the planes XY and YZ and on the input, output according the picture 6. In the plane XY, the measuring ran step by step with 10 cm distance in 7 surfaces. In the area of input, the distance of measuring points was reduced to 1 cm to reach the most accurate figures about the character of entrance flow field decomposition. In the plane YZ, six surfaces were measured with the step of 3 cm. The output of the laboratory box was properly measured in square raster 12 x 12 cm. At evaluation of entrance speed, the measuring had big effect on the construction of ventilator. Therefore about 50 point measurements were performed and the average value was evaluated as entrance speed of ventilator flow.

During the measurement of speed field in the box, in the plane XY and YZ, it was necessary to evaluate the flow speed in the three perpendicular axes (X, Y, Z). These three values were recalculated into form of final speed of flow by the quadratic sum (equation 9). At evaluation of measuring results, the program MATLAB2011b was used to display flow field in the individual planes (picture 7series).

$$\|v\| = \sqrt{v_x^2 + v_y^2 + v_z^2} \tag{9}$$

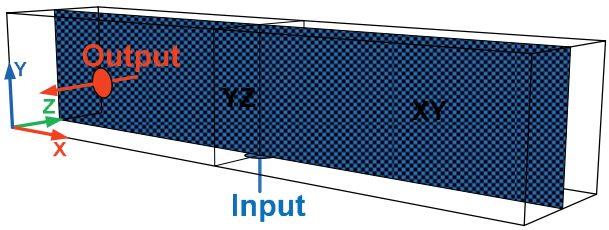

Figure 6. Measured area.

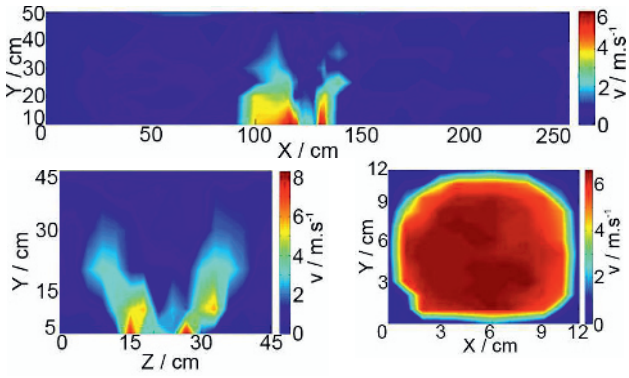

Figure 7. The results of measurement of the velocity field in the XY plane (top image), YZ plane (left image) and outlet hole (right image).

The character of entrance ventilator flow can be noted during the speed field of the flow in the plane XY and YZ. Ventilator creates turbulent rotating vortex that propagates to the sides and loses quickly its intensity. In the middle of the box, the flow intensity reaches almost the half value of maximal speed. (v_{max} = 8.4 m·s^{-1}).

Next, the attention was paid to the speed profile on the box exit. The maximal speed value of flow was approximately 6.6 m·s^{-1}.

5.2 Evaluation of results

At the comparison of measured results and simulated values, the average values of flow speed on input, output and planes XY, YZ for different turbulent models were compared.

The value of model k–ε RNG (in the table) suits best to the real measurement. This model corresponds to the real measurement in both planes, only with slights deviations. The method of result comparison using the average values can be considered as a tentative. The statistical analysis provides more accurate comparison of presumable results accordance. The method ANOVA (Analysis of variance) was chosen to the statistical evaluation. This method compares each measuring plane with the real measurement separately.

Table 3. Comparison of the average values of flow velocity.

velocity [m·s^{-1}]	input	output	plane XY	plane YZ
k-ε Standard	8.16	5.04	0.79	1.19
k-ε Realizable	8.16	4.94	0.96	1.35
k-ε RNG	8.16	5.25	1.01	1.54
k-ω Standard	8.16	4.94	0.81	1.17
k-ω SST	8.16	5.2	0.86	1.25
Real measurement	8.9	5.7	0.98	1.55

Table 4. Results of the analysis in the plane XY.

Height [cm]	k-ε Stan.	k-ε Real.	k-ε RNG	k-ω Stan.	k-ω SST
10	0.28	0.719	0.757	0.0729	0.805
20	0.7	0.6168	0.4638	0.0059	0.5569
25	0.6867	0.2471	0.3189	-	0.1955
30	0.7097	0.1551	0.9601	-	0.2188
35	0.35	0.26	0.9183	-	0.1321
45	0.4106	0.8434	0.6447	-	0.6839
50	0.0024	0.0693	0	-	0.0076
average	0.448486	0.415814	0.5804	-	0.3714
average	0.5227	0.4735	0.6771	-	0.4312

The table 4 displays the individual results using probabilistic accordance between measuring and simulated values. The probabilities of the biggest conformity for the individual levels are marked by gray backgrounds in the table. At the bottom of the table is the arithmetic average of the individual probabilities, the greatest probability of conformity with the measured value corresponds to the k-ε RNG model. The text highlighted by grey color representing the average of the values including the last level measured at a height of 50 cm. With regard to these values it is suitable to neglect the analysis results and to allow for the first six levels. So that the results aren't affected. For example of the model k-ε RNG that has the biggest accordance with the real measurement, up to 11% distortion would come about. On the following graphs, there are the results of comparison of model of k-ε RNG and other turbulent models towards the real measurement. The axis description of undermentioned graphs is following: axis x shows length of the box in range (0-250 cm), axis y shows the final flow speed according the equation (9).

6 Measurement and evaluation flow field with temperature transfer

6.1 Procedure and measuring results

The measurement for laboratory box went on the same way as during the previous example, but the difference was that the upper cover and the box were rotated about 180° so that the upper "empty" side represented the bottom of the box. The hot-air ventilators (Cata Empire CTH-5000) were used as a source for the real simulation of the thermal turbulence. Altogether, four hot-air ventilators were located under the open bottom of the box. The extraction ventilator is situated in the upper part to ensure better circulation of hot air.

The temperature measurement was watched and evaluated in the "specific" place in the box, as it is displayed on the picture 16. This place was chosen with regard on appropriate location of measuring probe (Voltcraft DL-181THP) using structural detail of the laboratory box. The measuring unit noted figures of temperature, pressure and relative humidity in each during 7 minutes. After all units were turned on, the temperature reached the maximal values of 50°C in 1 minute of measuring. Subsequently, the values start to fluctuate in the interval < 48, 50 °C > (picture 17).

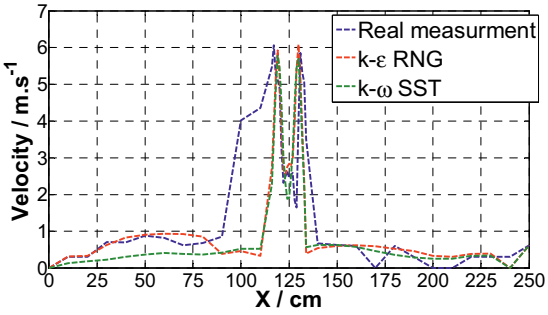

Figure 8. Comparison of measured and simulated data at a height of 10 cm.

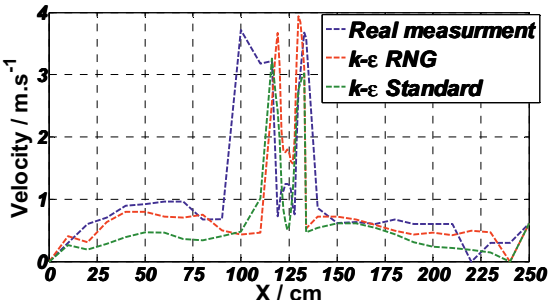

Figure 9. Comparison of measured and simulated data at a height of 20 cm.

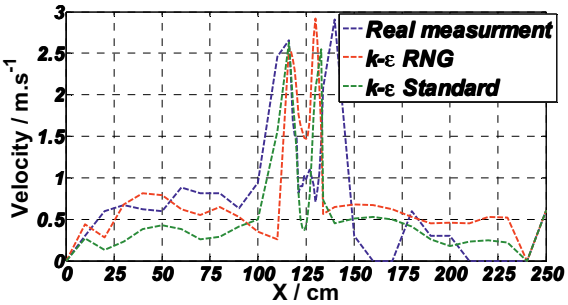

Figure 10. Comparison of measured and simulated data at a height of 25 cm.

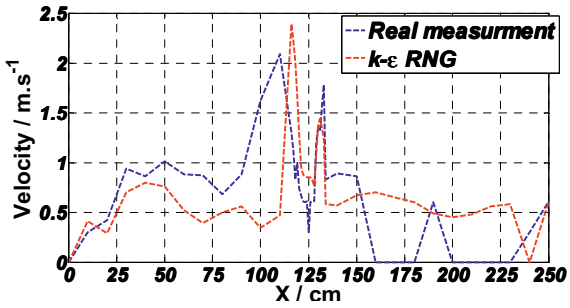

Figure 11. Comparison of measured and simulated data at a height of 30 cm.

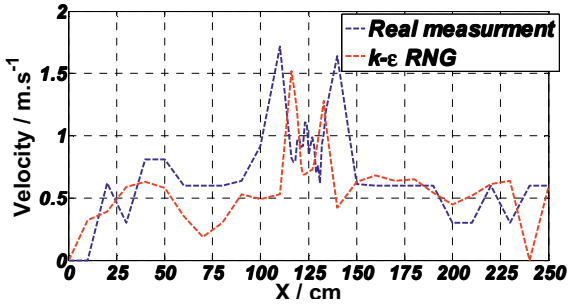

Figure 12. Comparison of measured and simulated data at a height of 35 cm.

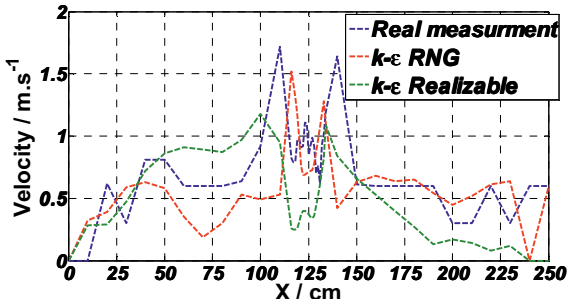

Figure 13. Comparison of measured and simulated data at a height of 45 cm.

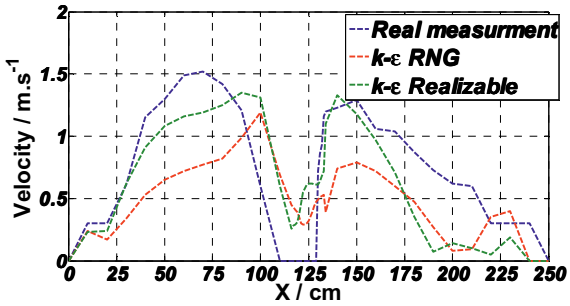

Figure 14. Comparison of measured and simulated data at a height of 50 cm.

Next, the measuring using thermal camera was performed, but it didn't develop into expected results, because the material of the box sides was excessive thermal insulators. The thermal camera showed demonstrable results during the measuring of temperature on the extraction ventilator, where the maximal temperature achieved approximately 55 °C, and on the exit of hot-air ventilator, the maximal temperature achieved 250 °C (523 K).

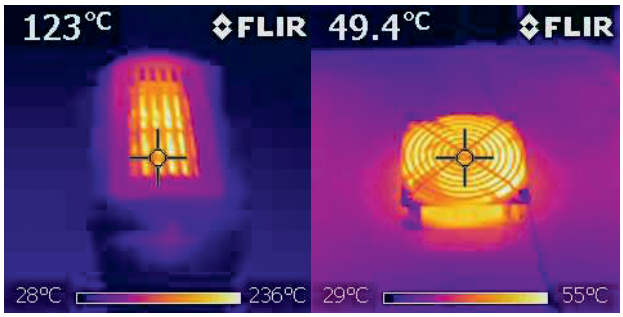

Figure 15. Images of the thermal camera for measure the temperature of the hot-air ventilator (left) and output fan (right).

6.2 Evaluation of results

The results of the final simulation are in a very good accordance with the real measurement. Temperature in the box moved in the range <54.2, 58.7 °C> during the simulation. In the measured place (see picture 16) the temperature of simulation is in the range <49.7, 54.2 °C>, that complies with the measured values. The maximal temperature on the extraction ventilator was 53.85°C during the simulation, this temperature correspondents to result of measurement with thermal camera (picture 15).

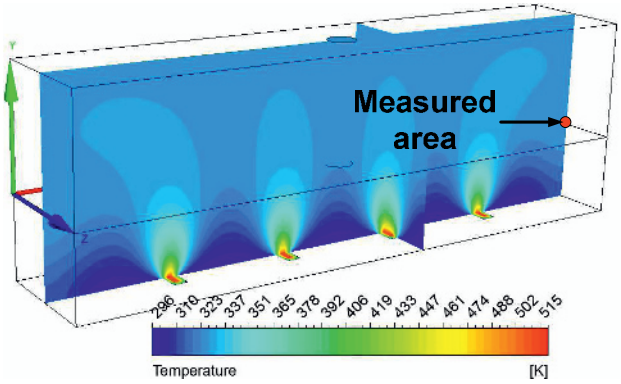

Figure 16. Distribution of temperature field in the box.

Time for which the temperature in the measuring point achieves 50°C was also monitored.

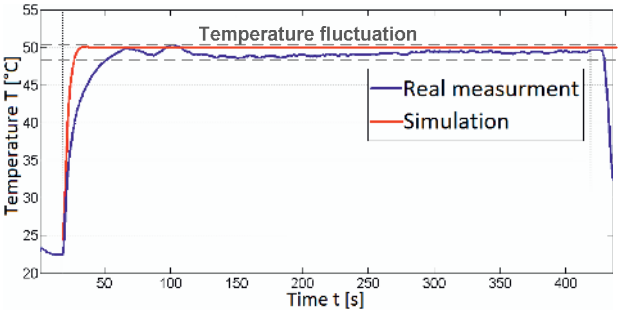

Figure 17. Time dependence of the temperature rise.

At the beginning of the real measurement (blue-marked on the picture 17), there is a curved line (approximately linear) which depicts temperature in the room. After the

hot-air ventilators were turned on, the temperature starts to rise logarithmically to T ≈ 50 °C, on the value T ≈ 49 °C the temperature stabilize with noticeable fluctuations. The temperatures of measurement and simulation are equal with the minimal deviation, the biggest difference was in time when the temperature in the box achieves the maximal value. The time of heating to maximal temperature was for simulation t_{max} ≈ 20s and for real measuring t_{max} ≈ 60 s. This time difference could be compensated by setting the peripheral conditions, but the time doesn't matter for this simulation.

Therefore there is the possibility to provide laboratory box with the more exhaust ventilators, finally the comparison between example with one extraction ventilator and three extraction ventilators was done. On the picture 18 and 19, there are streamlines of air from hot-air ventilators to the extraction ventilators. The result of this simulation displays that in the case of using one extraction ventilator the power of side hot-air ventilators are limited by the ventilators in the middle of the box. In the case of using three extraction ventilators, the flow field is spread so that all hot-air ventilators heat equally the space in the box.

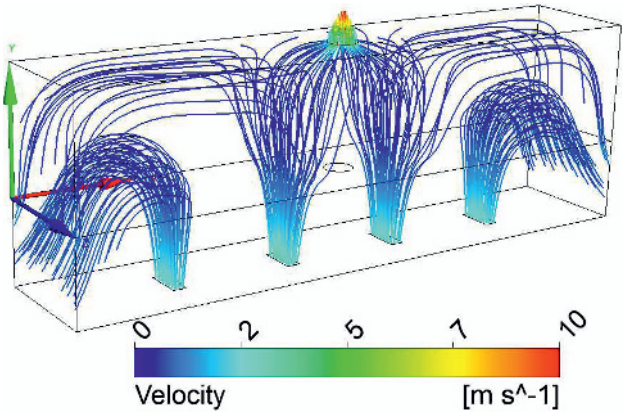

Figure 18. The flow of hot air in the box with one extraction ventilator.

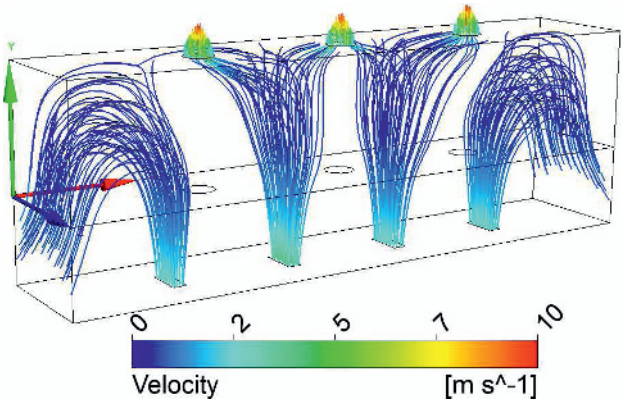

Figure 19. The flow of hot air in the box with three extraction ventilators.

7 Conclusions

In this article, the team of authors focused on the modeling of air flow in the simulated box. Then the model was defined using the measured figures and the results of simulation from the program ANSYS Fluent 14 were compared to the real data. On the basis of the statistical method ANOVA the numerical model was chosen, this model correspondents the best to the real measurement. In the first part the different turbulent models were defined without the equation of energy.

In the second part the mathematical model was widened by the modeling with the temperature transfer.

The final results are in a good accordance compared to experimental measurement.

Acknowledgements

The research was supported by the following grant projects: the Technology Agency of the Czech Republic, project No. TA01020932, the Czech Science Foundation, project No. GAP108/11/1057, the Ministry of the Interior, project No. VG20102015053. The work on this project was supported by the Grant Agency of VSB-Technical University of Ostrava, grant No. SGS SP2013/69 and SP2012/55. The research has been partially supported by the project No. CZ.1.07/2.3.00/20.0217 "The Development of Excellence of the Telecommunication Research Team in Relation to International Cooperation" within the frame of the operation programme "Education for competitiveness" financed by the Structural Funds and from the state budget of the Czech Republic.

References

1. T., David, J., Latal, F., Hanacek, P., Koudelka, J., Vitasek, P., Siska, J., Skapa, V., Vasinek, *Advances in Electrical and Electronic Engineering*, **9**, 179-186 (2011)
2. O., Wilfert, H., Henniger, Z., Kolka, *Proceedings of SPIE - The International Society for Optical Engineering 7141*, (2008).
3. A. K., Majmudar, J. C., Ricklin, *Free Space Laser Communications Principles and Advances*, (2008)
4. M., Kozubkova, *Modeling of fluid flow: FLUENT, CFX*. **1** (2008)
5. T., Blejchar, *Turbulence – Flow modeling - CFX*. **1** (2010)
6. M., Kozubkova, and S., Drábková. *Numerical modeling of flow: FLUENT I*. **1** (2003)
7. SAS IP, Inc. *ANSYS FLUENT: Theory Guide. Release 14.0.* (2011)
8. M., Kozubkova, T., Blejchar, M., Bojko, *Modelling of heat, mass transfer and momentum.* **1** (2011)